Anticipating the induced delamination formation in composite laminates subjected to bending loads

Mohammad Bahrami[1], Mohsen Malakouti[1], Amin Farrokhabadi[1*]

[1]Department of Mechanical Engineering, Tarbiat Modares University, Tehran, Iran

Abstract

In this research, the effects of induced delamination on the variation of the mechanical properties of composite laminates subjected to bending loads are investigated using a micromechanical model. For this purpose, the variation of the mechanical properties of delaminated laminates is determined using stress analysis of damaged ply and classical laminate theory (CLT) relationships. Using the proposed model and CLT, the fracture toughness due to induced delamination formation is presented in cross-ply laminates. Subsequently, the variation of strain energy release rate (SERR) is calculated in terms of crack density using analytical and finite element models to detect dominant failure modes in different crack densities. The results are compared with those of matrix cracking propagation. The results obtained by the proposed analytical model are in good agreement with those obtained by existing numerical and experimental approaches. The proposed model can be utilized to predict induced delamination formation in composite laminates subjected to bending loads.

Keywords: Induced delamination, Micromechanical model, Fracture toughness, Strain energy release rate, Bending loads

Nomenclature

[1] * Corresponding Author, Email Address: amin-farrokh@modares.ac.ir

θ : Rotation

k : Curvature

ν : Poison ratio

ρ : Crack density

η_x : Shear to longitudinal tension mutual coefficient

η_y : Shear to transverse tension mutual coefficient is given by

$D(\rho, l_d)$: Damage parameter

EI :Flexural stiffness

$G(\rho)$: SERR in the presence of a matrix crack

$G(\rho, l_d)$: SERR in the presence of delamination

G_{del} : Fracture toughness corresponding to delamination initiation

G_{mc} : Fracture toughness due to matrix cracking formation

L_d : Delamination length

M : Bending moment

1. Introduction

In recent years, the application of composite laminates has considerably been increased in numerous industries. This is due to the unique properties of these materials, including the high strength-to-weight ratio compared to other materials, such as metal alloys.[1] However, it is necessary to consider the impact of diverse damage modes in these materials in the initial design phases because these damages mechanisms result in a reduction in the structure's load-carrying capacity and, ultimately, they accelerate the final failure.[2] Delamination is one of the most important damage modes that threaten composite laminates.[3] The low interlaminar fracture toughness and out-of-plane strength of the composite laminates causes the matrix cracks to grow along the ply thickness direction and reach the ply boundary and finally the induced delamination is formed.[4] Subsequently, by increasing loading, the induced delamination grows, leading to the failure of the composite laminate. In recent years, many studies have been conducted to achieve a deeper understanding of the nature of induced delamination and the factors affecting it to be applied for predicting this dangerous phenomenon, hence preventing a reduction in the performance of composite structures and increasing their lifetime under different operating conditions. By employing an approximate stress function Nairn and Hu[5] analyzed the induced delamination in composite laminates using the Variational method. In another study, Armanios *et al.*[6] investigated the formation of matrix cracking and induced delamination using an analytical model by considering the effects of hygrothermal stresses. Comparing their results with the experimental results showed that this model could predict the critical load and delamination growth. Fukunaga *et al.*[7] used a one-dimensional shear-lag model to examine the response of cross-ply laminates containing delamination. The results indicated that the strain of matrix crack initiation only depends on the thickness of 90º lamina, however it was observed the ultimate failure strain is independent of this parameter. Dharani and Tang[8] used a shear-lag micromechanical model in their research. According to the results, samples in which the 90º lamina had a larger thickness exhibited a larger tendency for delamination formation. Kashtalyan and Soutis[9-11] employed the shear-lag and ECM methods to study the stiffness degradation in delaminated cross-ply laminates. In another study, Pupurs *et al.*[12] used the effective stiffness of the damaged layer in the form of CLT to calculate bending stiffness of cross-ply composite laminates containing matrix cracks in 90º plies and delamination at the interface of 0º/90º. They compared the results of this method with those obtained by FE model of the four-point bending

test. Miami *et al.*[13] investigated the relationship between the force exerted on the composite laminate with increase in the matrix crack density and delamination length using the analytical method and compared their results with experimental outcomes. Using fracture mechanics concept, Zubillaga *et al.*[14] presented a criterion to evaluate the formation of induced delamination in composite laminates. This criterion was developed based on calculating the strain energy release rate (SERR) required for delamination propagation which was compared with fracture toughness at the 0º/90º interface. In another study, Zubillaga *et al.*[15] confirmed the failure criterion presented in Ref. 14 via experimental tests. París *et al.*[16] used the Boundary Element Method (BEM) to study the initiation and growth of delamination in cross-ply laminates in the presence of thermal stresses. Sosa and Karapurath[17] presented a novel method based on the extended FE method (XFEM) to model delamination in cross-ply laminates. Their results indicated that an increase in stress at 0º/90º interface, which is usually the main causes of the delamination, entails reducing SERR. Abdullah *et al.*[18] used XFEM to investigate matrix cracking and induced delamination in Carbon Epoxy composite laminates. The basis of their method of study was the use of volume element to predict stress-inducing delamination. Tay *et al.*[19] used XFEM and cohesive elements to examine matrix cracking and induced delamination in composite laminates and validated their results with the experimental results. Farrokhabadi *et al.*[20,21]used a micromechanical method to calculate the SERR required for matrix cracking propagation and induced delamination in composite laminates and compared their results with numerical results. In another research, Farrokhabadi *et al.*[22] used an analytical model to examine the variation of mechanical properties of composite laminates containing matrix cracks under bending loads. Moreover, they determined the fracture toughness in composite laminates containing matrix cracks. Bahrami and Farrokhabadi[23] proposed a micromechanical model which was capable of providing the bending moment required for matrix cracking propagation in cross-ply composite laminates. Moreover, the variation of SERR in cross-ply laminates containing matrix cracks was presented in terms of the crack density. Hajikazemi *et al.*[24] introduced a Variational model capable of predicting displacement/stress fields and the effective thermo mechanical properties of composite laminates with matrix cracks at non-uniform distances subjected to bending loads. Mortell *et al.*[25] combined micromechanical testing and acoustic emission to study the delamination length in cross-ply composite laminates. Their results indicated a linear relationship between delamination length and the applied force imposed to the

samples. By employing the CZM method and experimental tests, Turon *al.*[26] investigated the effects of various parameters, such as the interfacial strength and mixed-mode interaction on the maximum load inducing delamination in composite laminates. Hallett *et al.*[27] proposed a numerical modeling for the accurate prediction of matrix crack and delamination damage mechanisms and compared the obtained results with experimental tests. Turon *et al.*[28] examined the delamination propagation in composite laminates using a thermomechanical model and experimental tests. Fotouhi *et al.*[29] investigated the critical load leading to delamination initiation and growth using the sentry function. The results showed that this function is capable of predicting delamination formation with high accuracy. Furthermore, Saeedifar *et al.*[30] used acoustic emission (AE) to calculate the critical fracture toughness leading to the onset of delamination in various lay-ups of Glass/Epoxy composite laminates. The results obtained by this method were in good agreement with the fracture toughness obtained from experimental tests.

Reviewing the before mentioned studies indicates that the variation of mechanical properties of general composite laminates containing delamination subjected to bending loads has not been studied so far. Therefore, developing an analytical micromechanical model capable of predicting the variation of mechanical properties, including flexural modulus, Poisson's ratio, longitudinal shear to tension mutual coefficient, and transverse shear to tension mutual coefficient for any stacking sequence, is among the aims of this research. Subsequently, using CLT, the fracture toughness required to formation of induced delamination in composite laminates has been estimated, which has not been performed in previous research works. Finally, using the FE method, numerical model have been introduced to predict SERR in terms of the crack density in cross-ply laminates subjected to bending loads containing matrix cracks and delamination.

2. Methodology

2.1. Delamination due to transverse matrix cracking

In composite laminates containing 90° lamina subjected to bending loads, the matrix cracking in the 90° lamina grows and reaches the interface of adjacent plies. Increasing the load causes the formation of induced delamination at the ply interface. Fig. 1 depicts a composite laminate containing a matrix crack with a crack density of $\rho_1$and a delamination with a length of$2L_d$.

After the formation of delamination in the composite laminate, in 90° lamina, due to creation of the dead zone, area region with the zero stresses and length of $2L_d$ will be made. As a result, this zone can be skipped, and a unit cell with the length of ($L-2L_d$) can be considered in 90° ply.

2.2. Calculation of the strain energy release rate due to matrix cracking and induced delamination

The strain energy release rate in a laminate subjected to bending moment can be expressed as follows:[20]

$$G = \frac{M^2}{2}\frac{dC_B}{dA} \tag{1}$$

Where $C_B = \frac{\theta}{M}$ and dA represents the cracked region. The rotation θ in terms of the curvature κ is as:

$$\theta = \kappa L \tag{2}$$

Where L is the ply length. Eq. (1) can be expressed as follows:

$$G = \frac{M^2 L}{2}\frac{d(\frac{\kappa}{M})}{dA} \tag{3}$$

Where $\frac{\kappa}{M} = \frac{1}{EI}$.

According to Fig. 2. it is assumed that composite laminate which is subjected to a bending moment contains matrix cracks with a crack density of ρ_1. This unit cell is prone for the formation of next matrix crack with the density of ρ_2.

In this case, assuming a constant bending moment M exerted on composite laminate, the SERR in the presence of a matrix crack that its density increases from the first state (1) to the second state (2) is obtained as

$$G(\rho) = \frac{\frac{M^2 L}{2}\left[(\frac{1}{E(\rho_2)I}) - (\frac{1}{E(\rho_1)I})\right]}{t_{90} \times w} \tag{4}$$

Where, L is the unit cell length, E(ρ) is the flexural modulus of laminate in the presence of matrix cracking, I is the moment of inertia, and t_{90} and w are the thickness and width of the 90° ply, respectively. Moreover, according to Fig. 3. for the considered composite laminates

subjected to bending loads containing a matrix crack with a crack density ρ_1, one another probable scenario is the formation of delamination with a length $2L_d$ which is originated from the matrix crack tip. In this case, the SERR in the presence of delamination is determined as

$$G(\rho,l_d)=\frac{\frac{M^2L}{2}\left[\left(\frac{1}{E(\rho,l_d)I}\right)-\left(\frac{1}{E(\rho)I}\right)\right]}{2L_d\times w} \tag{5}$$

Where $2L_d$ denotes the delamination length.

Assuming that a composite laminate is subjected to a four-point bending loading which is prone for the formation of matrix cracking and induced delamination. In continue, a relationship is introduced to determine the fracture toughness due to induced delamination formation. According to Fig. 4. the bending moment M can be written in terms of the applied transverse force for the four-point bending test as

$$M=\frac{F}{2}\times L_1 \tag{6}$$

Where L_1 is the arm length. According to Eqs. (4) and (5), it can be concluded that

$$M^2G_{unit}(\rho)=\begin{cases}G(\rho)\\G(\rho,l_d)\end{cases} \tag{7}$$

By substituting the moment M in Eq. (7) and using the energy criterion for the crack initiation, it can be concluded

$$\frac{F^2L_1^2}{4}G_{unit}(\rho)=\begin{cases}G(\rho)\\G(\rho,l_d)\end{cases} \tag{8}$$

Where $G(\rho,l_d)$ represents the fracture toughness corresponding to delamination initiation in the four-point bending test. In the four-point bending test, by recording the occurrence of delamination at different forces, one can determine the left-hand side of Eq. (8) using which one can calculate the interlaminar fracture toughness induced by delamination. It should be note that, to calculate $E(\rho)I$ or $E(\rho,l_d)I$, the relationships developed by Farrokhabadi *et al.*[20] are used, where the reduced material properties are calculated as

$$\begin{gathered}\frac{1}{E_x}-k^2\frac{D(\rho,l_d)}{E_y}=\frac{1}{E_x(\rho,l_d)},\ \frac{\nu_{yz}}{E_y}-k'\frac{D(\rho,l_d)}{E_y}=\frac{\nu_{yz}(\rho,l_d)}{E_y(\rho,l_d)},\ D(\rho,l_d)=\frac{E_y}{E_y(\rho,l_d)}-1,\\ \frac{1}{E_z}-k'^2\frac{D(\rho,l_d)}{E_y}=\frac{1}{E_z(\rho,l_d)},\ \frac{\nu_{xz}}{E_x}-kk'\frac{D(\rho,l_d)}{E_y}=\frac{\nu_{xz}(\rho,l_d)}{E_x(\rho,l_d)},\ \frac{\nu_{yx}}{E_y}-k\frac{D(\rho,l_d)}{E_y}=\frac{\nu_{yx}(\rho,l_d)}{E_y(\rho,l_d)},\end{gathered} \tag{9}$$

Where k, k' are ply constants dependent of the damage parameter ρ [20]. Besides, $D(\rho,l_d)$ is macroscopic damage parameter. Having the properties of the damaged lamina, one can calculate the variation of properties of the composite laminates due to induced delamination as

$$E_x(\rho,l_d)=\frac{12}{d_{11}(\rho,l_d)H^3} \tag{10}$$

$$\upsilon_{xy}(\rho,l_d)=-\frac{d_{12}(\rho,l_d)}{d_{11}(\rho,l_d)} \tag{11}$$

Where H is the total thickness of laminates. Additionally, shear to longitudinal tension mutual coefficient is given by:

$$\eta_x(\rho,l_d)=-\frac{d_{13}(\rho,l_d)}{d_{11}(\rho,l_d)} \tag{12}$$

And the shear to transverse tension mutual coefficient is given by:

$$\eta_y(\rho,l_d)=-\frac{d_{23}(\rho,l_d)}{d_{11}(\rho,l_d)} \tag{13}$$

The analytical model is capable to determine the SERR required for matrix cracking propagation and delamination initiation using Eqs (4) and (5). Given the limitation of previous study, in the following, a finite element model is presented, which compares the variation of SERR due to matrix cracking propagation and delamination with the proposed analytical model to verify the analytical results.

2.3. Numerical modeling

2.3.1. Numerical simulation of the four-point bending test for cross-ply laminates

In this section, the aim of presenting the finite element model is to extract SERR in cross-ply composite laminates$[90/0]_s$and $[90_2/0_2]_s$. Fig. 5. represents the geometry of the finite element model. This model is composed of three plies with a length of L=30 mm. The distance between the loading points is 10 mm, and the sample's width is 0.8 mm. This laminate is subjected to four-point bending load with an exerted force of 20 N. The region containing the matrix crack and delamination is between loading points. The simply supported boundary conditions are used for numerical simulation. In detail, the nodes at the lower edge of the sample at x=0,

displacement in x and y direction are constrained whereas nodes at the lower edge of the sample at x=L are constrained only in y-directions. Since only the 90^0 ply subjected to tension contains matrix cracking and delamination, symmetrical modeling along the thickness direction is impossible. The element used to model the plies is the reduced-order, three-dimensional, 8-node element (C3D8R). Moreover, to increase the accuracy of output results, the mesh size in the middle section (damaged area) of the sample is smaller than those in its other sections.

The first step in finding the SERR is to calculate the bending stiffness. Having the force exerted on the sample and calculating the bending moment M_x using Eq. (6) this parameter is given by:

$$E(\rho) I = w \frac{M_x}{k_x} \tag{14}$$

In this relationship, w and k_x are the width and curvature of the beam, respectively. After computing the laminate's bending stiffness in the presence of matrix crack and delamination states for various damage densities, the SERR can be calculated. To calculate SERR corresponding to the matrix crack, it is sufficient to substitute the bending stiffness at every crack density (second state) and the previous crack density (first state) in Eq. (4). Moreover, Eq. (5) has been used to calculate the strain energy release rate due to delamination. For this purpose, one must substitute the bending stiffness corresponding to delamination and matrix cracking in the first and second states, respectively, for each damage density. In these relationships, L is the length of the middle section of the beam and is equal to 10mm.

3. Results and discussion

3.1. Model validation

First, the micromechanical model in Fig. 6. is validated based on the research conducted by Pupurs *et al.*[12] As seen in Fig. 6. The obtained analytical results has good agreement with the finite element results.[12] This indicates that the proposed model can be used for the variation of other properties of delaminated composite laminates subjected to bending loads. The mechanical properties were listed in Table 1.

3.2. Variation of properties of delaminated composite laminates subjected to bending loads

Figs. 7-9. display the variation of flexural properties of composite laminates subjected to bending load as a function of different crack density as well as delamination length. It should be noted that, for the analysis, the length of induced delamination is considered equal to 0.1 and 0.5 times the thickness i.e., l_d=0.1 and 0.5.

According to Fig. 7a and c, the longitudinal flexural modulus decreases by increasing the crack density in the two considered composite laminates. The bending modulus reduction induced by delamination is higher than those induced by the matrix cracking propagation, indicating that delamination has a more damaging impact on the laminate subjected to bending loads. Moreover, the longitudinal flexural modulus suffers a larger reduction by increasing the delamination length, indicating that an increase in delamination length leads to serious damage in composite laminates. Comparison of Fig. 7a and c show that longitudinal flexural modulus in laminate $[90_2/0_2]_s$ is much larger than laminate $[0_2/90_2]_s$ due to the presence of two 90° plies at the tensile side of the former laminate. In addition, according to Fig. 7b and d, the Poisson's ratio undergoes a quasilinear reduction. The reduction in Poisson's ratio due to delamination is larger than those induced by matrix cracking propagation, which is compatible with the problem physics. An increase in delamination length leads to a larger reduction in Poisson's ratio, which is more tangible in laminate $[90_2/0_2]_s$. The longitudinal flexural modulus reduction in laminate $[90/30_2]_s$ can be seen in Fig. 8a. By increasing the delamination length, the longitudinal flexural modulus reduction with respect to crack density increases. The bending modulus reduces by 8.12% for matrix cracking, 8.4% for delamination with l_d= 0.1, and 8.7% for l_d= 0.5. Fig. 8b. displays a reduction in Poisson's ratio in terms of crack density. The smallest reduction, equal to 33%, corresponds to matrix cracking, and the largest reduction, equal to 38.1%, corresponds to delamination with l_d=0.5. According to Fig. 8c. with increasing the crack density, the longitudinal coupling coefficient exhibits an enhancing trend. In addition the formation of induced delamination intensifies the rising trend of mutual coefficient. According to the figure, the smallest rise in the longitudinal coefficient, equal to 15%, corresponds to matrix cracking, and the largest rise, equal to 21%, corresponds to delamination with l_d= 0.5. According to Fig. 8d. changes in the transverse coupling coefficient increase pseudo-linearly with respect to the crack density. An increase in this mechanical parameter becomes stronger by increasing the delamination length. As can be seen, this parameter has increased by 24.8% for delamination

with l_d= 0.5. The variation of properties of a laminate lay-up $[60/-60]_s$ is also shown in Fig. 9. According to Fig. 9a. the longitudinal flexural modulus reduction for the matrix cracking and delamination with a length of l_d=0.5 is 22% and 26%, respectively. The reason for the increased reduction in the modulus can be due to the presence of both 60° and -60° plies containing matrix cracks on the tensile side of the laminate subjected to bending. In addition, Fig. 9b. shows that Poisson's ratio decreases up to a crack density of 0.2, after which it exhibits ascending behavior. According to the figure, the larger the delamination length is, the more the slope of Poisson's ratio will increase, which is a sign of instability of the laminate.

3.3. Fracture toughness required to delamination initiation

Using Eq. (5) and the experimental results in Ref. 25, which presents the force required for delamination initiation and propagation in cross-ply composite laminates, the fracture toughness corresponding to delamination initiation in cross-ply laminates subjected to bending loads has been calculated to be $G_{mc}=600\,30\frac{J}{m^2}$. It must be noted that the Farrokhabadi *et al.*[22] have used a similar method to extract the fracture toughness due to matrix cracking formation in cross-ply laminates, the value of which is $G_{mc}=231\,30\frac{J}{m^2}$. Subsequently, the validity of the calculations to determine the fracture toughness corresponding to delamination initiation is evaluated using the existing relationships. Now, in this section, the required force for delamination initiation at every crack density is calculated and compared with the presented experimental results in Ref. [25].

According to Table 2, the force required for matrix cracking propagation is less than that for delamination initiation up to the 12th, 7th, and 6th in lay-ups $[90_2/0_7/90_2]$, $[90_3/0_7/90_3]$, and $[90_4/0_7/90_4]$, respectively. Therefore, until the mentioned crack numbers, matrix cracking occurs which is followed by induced delamination in the next loading steps. Table 2 shows that the force required for matrix cracking propagation in the 13th, 8th, and 7th crack in $[90_2/0_7/90_2]$, $[90_3/0_7/90_3]$, and $[90_4/0_7/90_4]$, respectively, which is calculated using Eq. (8) and compared with the force required for delamination propagation. The results indicate that at this number of crack, delamination is dominant and occurs after the mentioned crack numbers. Comparing the results

of the presented micromechanical model with experimental results[25] indicates the accuracy of the analytical model in calculating the fracture toughness required to initiate delamination.

3.4. Finite element model

3.4.1. Variation SERR in bending load

After calculating the stiffness reduction due to matrix cracking and delamination, in this section, the variation of SERR as a function of crack density and induced delamination length, obtained using analytical and numerical model is represented for the cross-ply composite laminates, in Fig. 10. According to the obtained results, SERR has a descending behavior in the matrix cracking mode, whereas, in the delamination mode, it has an increasing trend. This is due to the instability of the laminate in the delamination mode. According to Fig. 10a. in $[90/0]_s$, laminate, the SERR due to matrix cracking is more than that due to delamination up to a crack density between 0.4 and 0.6 and less. Therefore, matrix cracking occurs in this range, and from a crack density of 0.6 onward, the value of SERR due to delamination becomes dominant, and this damage mode appears in the composite laminate. Moreover, it can be seen in Fig. 10b. that in $[90_2/0_2]_s$, laminate the SERR due to matrix cracking is higher than that due to delamination up to a crack density between 0.2 and 0.4. Hence, matrix cracking is expected to occur in this range, and delamination occurs after the crack density of 0.4. Comparing the numerical model results with the analytical model shows that the presented analytical model can provide the variation of the SERR at different track densities. It must be noted that the disagreement between the numerical and analytical results at some crack densities is mainly due to differences between the stiffness values obtained in the numerical and analytical results.

Conclusions

In this research, the variation of mechanical properties of composite laminates, including the flexural modulus, Poisson's ratio, and longitudinal and transverse coupling coefficients induced by matrix cracking and delamination were presented using a comprehensive micromechanical model. In addition, the fracture toughness corresponding to delamination initiation in cross-ply composite laminates was calculated using the proposed model and CLT. Using the obtained fracture toughness, the force required for delamination formation in each crack number was calculated and compared with the available experimental results. Finally, the variation of SERR

due to matrix cracking and delamination was calculated by presenting a finite element model and compared with the results of the analytical model. The proposed FE model is able to predict the range of crack densities in which matrix cracking or delamination occur. The acceptable agreement between the analytical results as well as the experimental and numerical results indicates the high capability of the proposed model in prediction of the affected material properties as well fracture toughness due to induced delamination formation.

References

1 De Finis R, Palumbo D, Galietti U. Evaluation of damage in composites by using thermoelastic stress analysis: A promising technique to assess the stiffness degradation. *Fatigue & Fracture of Engineering Materials & Structures.* 2020;43(9):2085-2100.

2 Madadi H, Naghdinasab M, Farrokhabadi A. Numerical investigation of matrix cracking propagation in cross−ply laminated composites subjected to three−point bending load using concurrent multiscale model. *Fatigue & Fracture of Engineering Materials & Structures.* 2020;43(6):1159-1169.

3 Venkatachalam S, Khaja Mohiddin S, Murthy H. Determination of damage evolution in CFRP subjected to cyclic loading using DIC. *Fatigue & Fracture of Engineering Materials & Structures.* 2018;41(6):1412-1425.

4 Brewer JC, Lagace PA. Quadratic stress criterion for initiation of delamination. *Journal of composite materials.* 1988;22(12):1141-1155.

5 Nairn J, Hu S. The initiation and growth of delaminations induced by matrix microcracks in laminated composites. *International journal of fracture.* 1992;57(1):1-24.

6 Armanios EA, Sriram P, Badir AM. Fracture analysis of transverse crack-tip and free-edge delamination in laminated composites. In: *Composite Materials: Fatigue and Fracture (Third Volume).* ASTM International; 1991.

7 Fukunaga H, Chou T-W, Peters P, Schulte K. Probabilistic failure strength analyses of graphite/epoxy cross-ply laminates. *Journal of composite materials.* 1984;18(4):339-356.

8 Dharani LR, Tang H. Micromechanics characterization of sublaminate damage. *International journal of fracture.* 1990;46(2):123-140.

9 Kashtalyan M, Soutis C. Analysis of composite laminates with intra-and interlaminar damage. *Progress in Aerospace Sciences.* 2005;41(2):152-173.

10 Kashtalyan M, Soutis C. Stiffness degradation in cross-ply laminates damaged by transverse cracking and splitting. *Composites Part A: Applied Science and Manufacturing.* 2000;31(4):335-351.

11 Kashtalyan M, Soutis C. Analysis of local delaminations in composite laminates with angle-ply matrix cracks. *International Journal of Solids and Structures.* 2002;39(6):1515-1537.

12 Pupurs A, Varna J, Loukil M, Kahla HB, Mattsson D. Effective stiffness concept in bending modeling of laminates with damage in surface 90-layers. *Composites Part A: Applied Science and Manufacturing.* 2016;82:244-252.

13 Maimı P, Camanho P, Mayugo J, Turon A. Matrix cracking and delamination in laminated composites. Part I: Ply constitutive law, first ply failure and onset of delamination. *Mechanics of materials.* 2011;43(4):169-185.
14 Zubillaga L, Turon A, Maimí P, Costa J, Mahdi S, Linde P. An energy based failure criterion for matrix crack induced delamination in laminated composite structures. *Composite Structures.* 2014;112:339-344.
15 Zubillaga L, Turon A, Renart J, Costa J, Linde P. An experimental study on matrix crack induced delamination in composite laminates. *Composite Structures.* 2015;127:10-17.
16 París F, Blázquez A, McCartney L, Mantič V. Characterization and evolution of matrix and interface related damage in [0/90] S laminates under tension. Part I: Numerical predictions. *Composites science and technology.* 2010;70(7):1168-1175.
17 Sosa JC, Karapurath N. Delamination modelling of GLARE using the extended finite element method. *Composites Science and Technology.* 2012;72(7):788-791.
18 Abdullah NA, Curiel-Sosa JL, Taylor ZA, Tafazzolimoghaddam B, Vicente JM, Zhang C. Transversal crack and delamination of laminates using XFEM. *Composite Structures.* 2017;173:78-85.
19 Tay T, Sun X, Tan V. Recent efforts toward modeling interactions of matrix cracks and delaminations: an integrated XFEM-CE approach. *Advanced Composite Materials.* 2014;23(5-6):391-408.
20 Farrokhabadi A, Hosseini−Toudeshky H, Mohammadi B. Damage analysis of laminated composites using a new coupled micro−meso approach. *Fatigue & Fracture of Engineering Materials & Structures.* 2010;33(7):420-435.
21 Farrokhabadi A, Hosseini-Toudeshky H, Mohammadi B. A generalized micromechanical approach for the analysis of transverse crack and induced delamination in composite laminates. *Composite Structures.* 2011;93(2):443-455.
22 Farrokhabadi A, Bahrami M, Babaei R. Predicting the matrix cracking formation in symmetric composite laminates subjected to bending loads. *Composite Structures.* 2019;223:110945.
23 Bahrami M, Farrokhabadi A. Propagation of Matrix Cracking and Induced Delaminatin in Cross-Ply Composite Beams Subjected to Bending Loads. *Mechanics of Advanced Composite Structures.* 2019;6(1):45-50.
24 Hajikazemi M, McCartney L, Ahmadi H, Van Paepegem W. Variational analysis of cracking in general composite laminates subject to triaxial and bending loads. *Composite Structures.* 2020;239:111993.
25 Mortell D, Tanner D, McCarthy C. In-situ SEM study of transverse cracking and delamination in laminated composite materials. *Composites Science and Technology.* 2014;105:118-126.
26 Turon A, Davila CG, Camanho PP, Costa J. An engineering solution for mesh size effects in the simulation of delamination using cohesive zone models. *Engineering fracture mechanics.* 2007;74(10):1665-1682.
27 Hallett SR, Jiang W-G, Khan B, Wisnom MR. Modelling the interaction between matrix cracks and delamination damage in scaled quasi-isotropic specimens. *Composites Science and Technology.* 2008;68(1):80-89.
28 Turon A, Camanho PP, Costa J, Dávila C. A damage model for the simulation of delamination in advanced composites under variable-mode loading. *Mechanics of materials.* 2006;38(11):1072-1089.

29 Fotouhi M, Pashmforoush F, Ahmadi M, Refahi Oskouei A. Monitoring the initiation and growth of delamination in composite materials using acoustic emission under quasi-static three-point bending test. *Journal of reinforced plastics and composites*. 2011;30(17):1481-1493.
30 Saeedifar M, Fotouhi M, Mohammadi R, Najafabadi MA, Toudeshky HH. Investigation of delamination and interlaminar fracture toughness assessment of Glass/Epoxy composite by acoustic emission. *Modares Mechanical Engineering*. 2014;14(4):1-11.

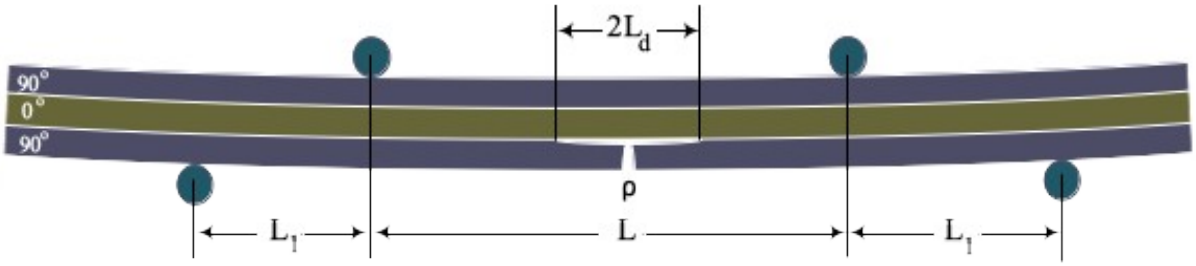

Fig. 1 Composite laminate containing a matrix crack with the density of ρ and induced delamination with length of $2\,L_d$

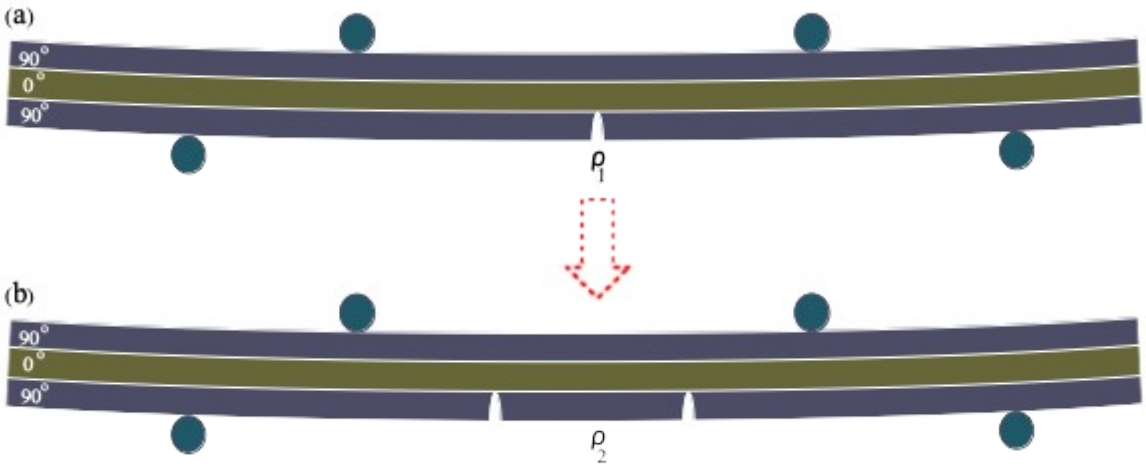

Fig. 2 The scenario representing matrix cracking propagation subjected to bending load; a) crack density of ρ_1, and b) crack density of ρ_2

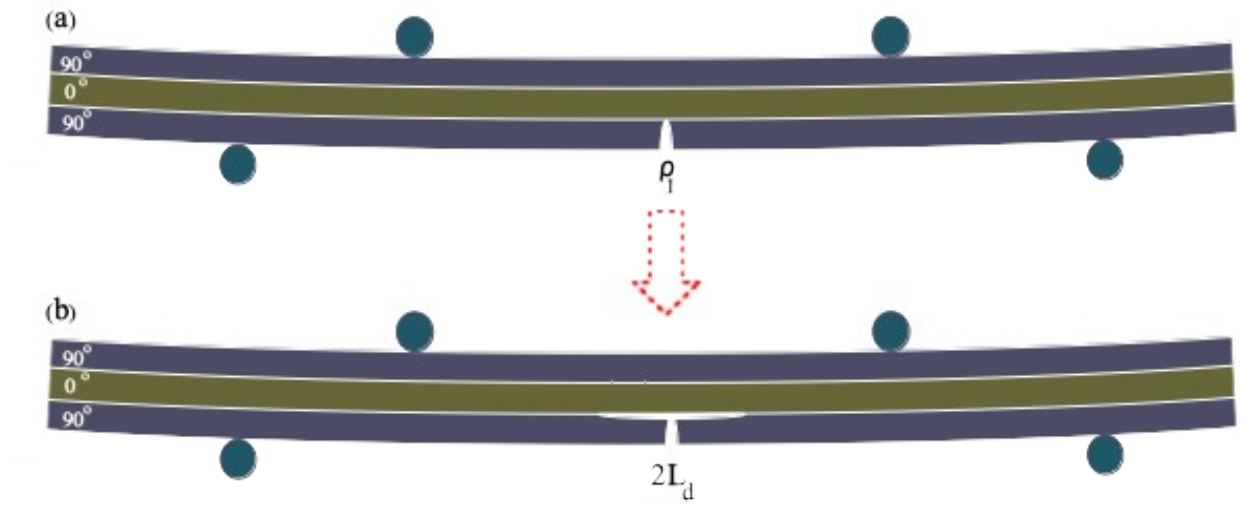

Fig. 3 The scenario representing delamination from at the tips of the matrix cracking; a) crack density of ρ_1, b) induced delamination with length of $2L_d$

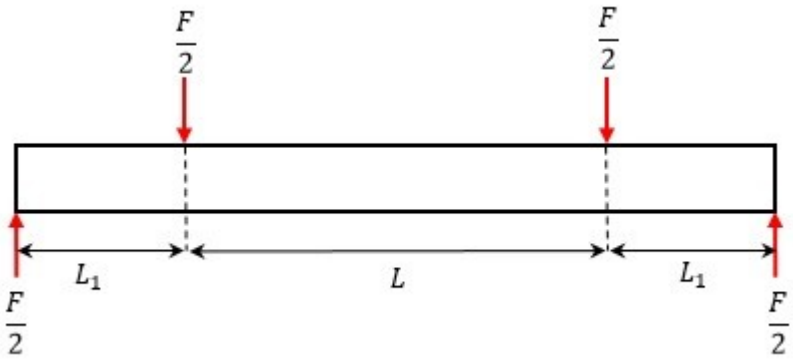

Fig. 4 Schematic representation of four-point bending test

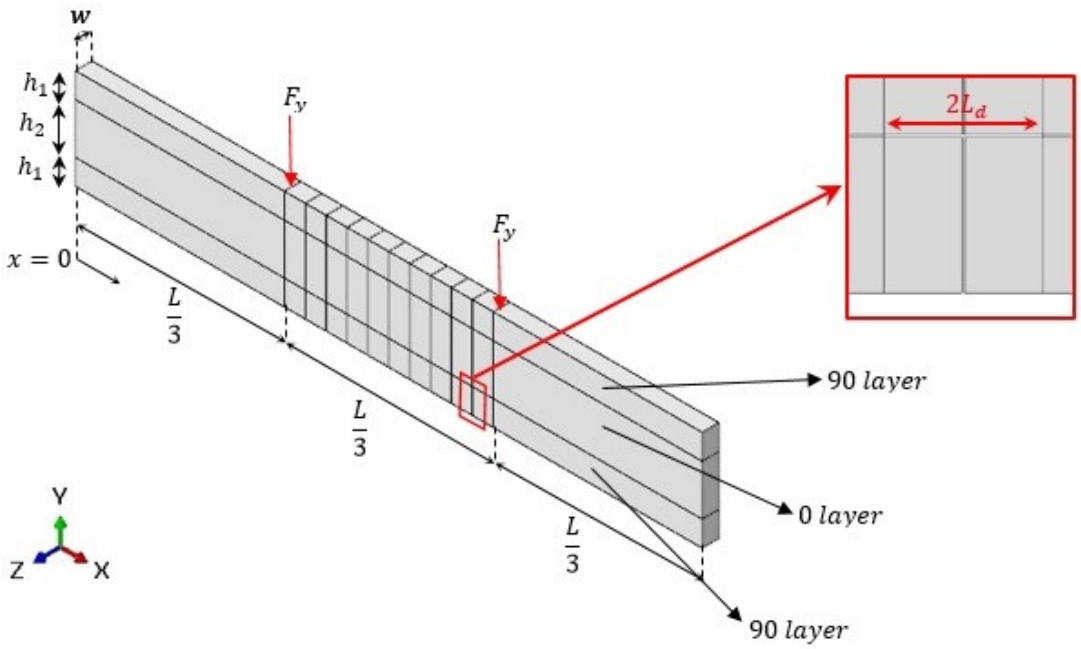

Fig. 5 The FE model used to calculate SERR in cross-ply composite laminates

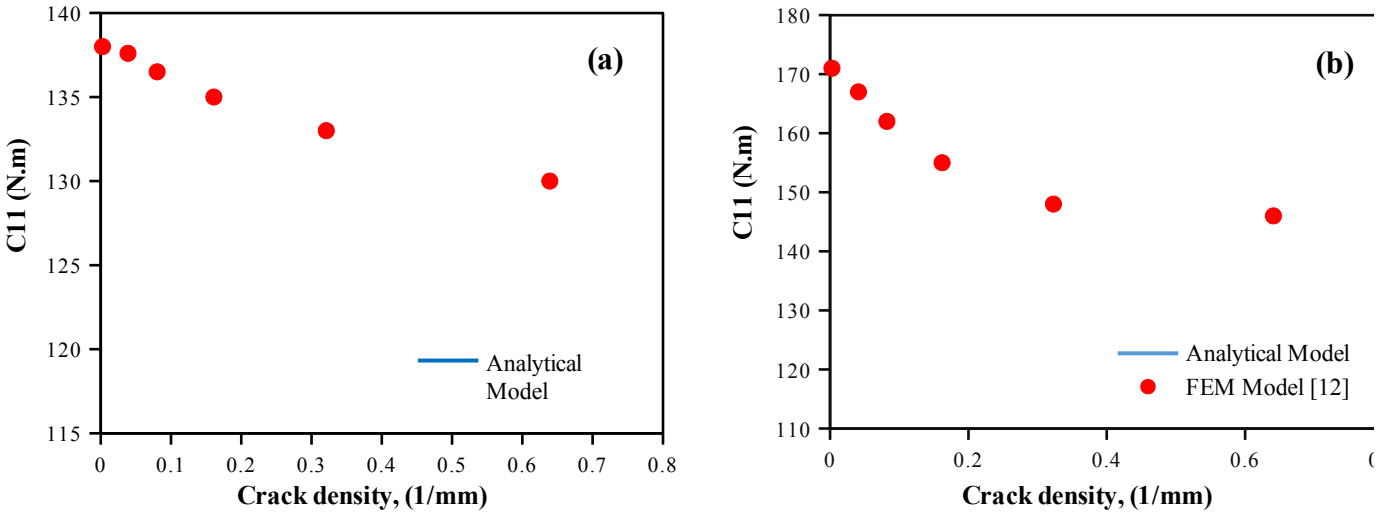

Fig. 6 Comparison of the bending stiffness reduction due to delamination formation (l_d=0.5) obtained by the analytical model and numerical model a) $[90/0_2]_s$, and b) $[90_2/0_2]_s$.

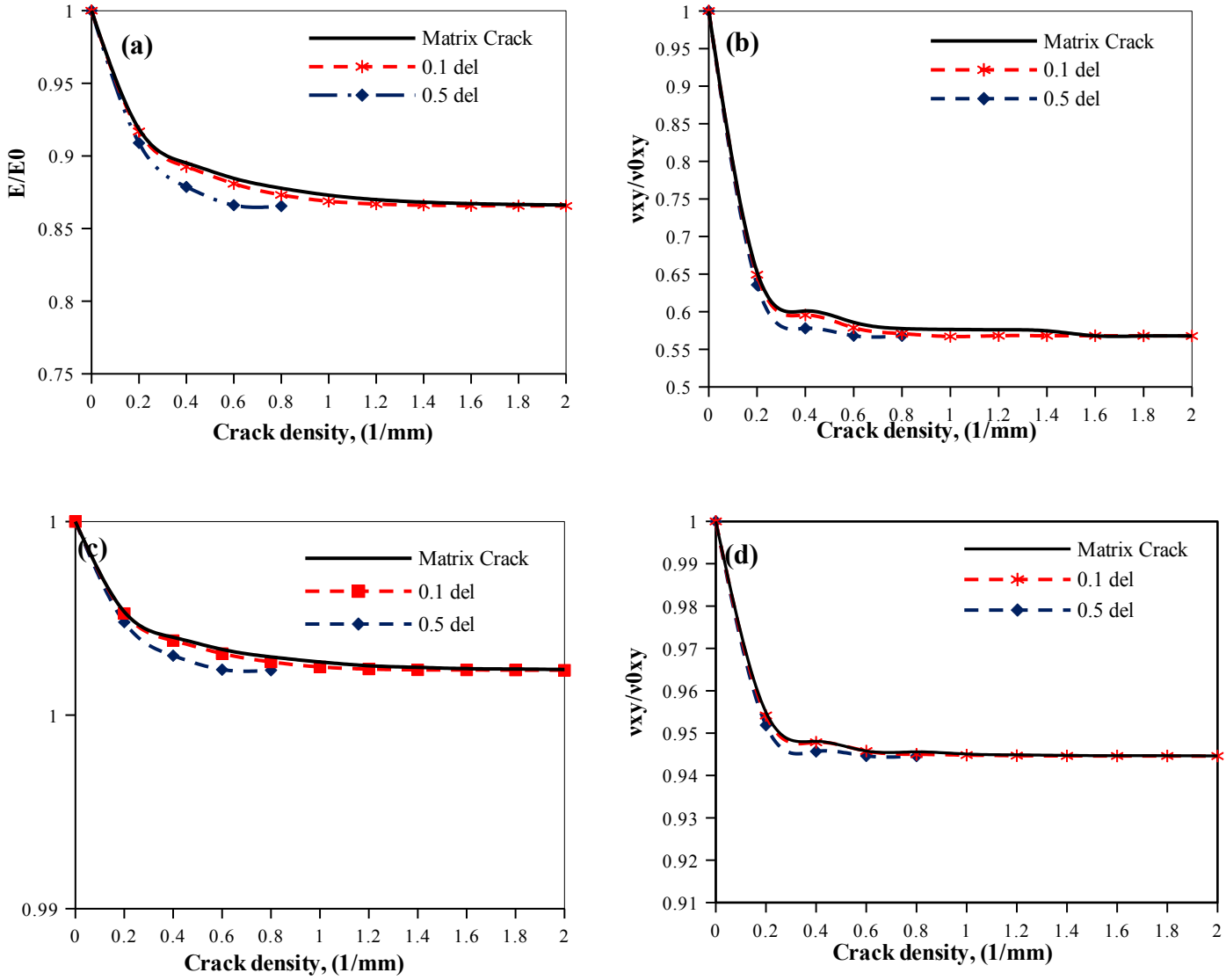

Fig. 7 Comparison of the variation of the properties due to matrix cracking and delamination with l_d= 0.1 and l_d=0.5 in cross-ply laminates subjected to bending loading; a) Longitudinal flexural modulus in cross-ply laminate $[90_2/0_2]_s$, b) Poisson's ratio in laminate $[90_2/0_2]_s$, c) longitudinal flexural modulus in laminate $[0_2/90_2]_s$, and d) Poisson's ratio in laminate $[0_2/90_2]_s$

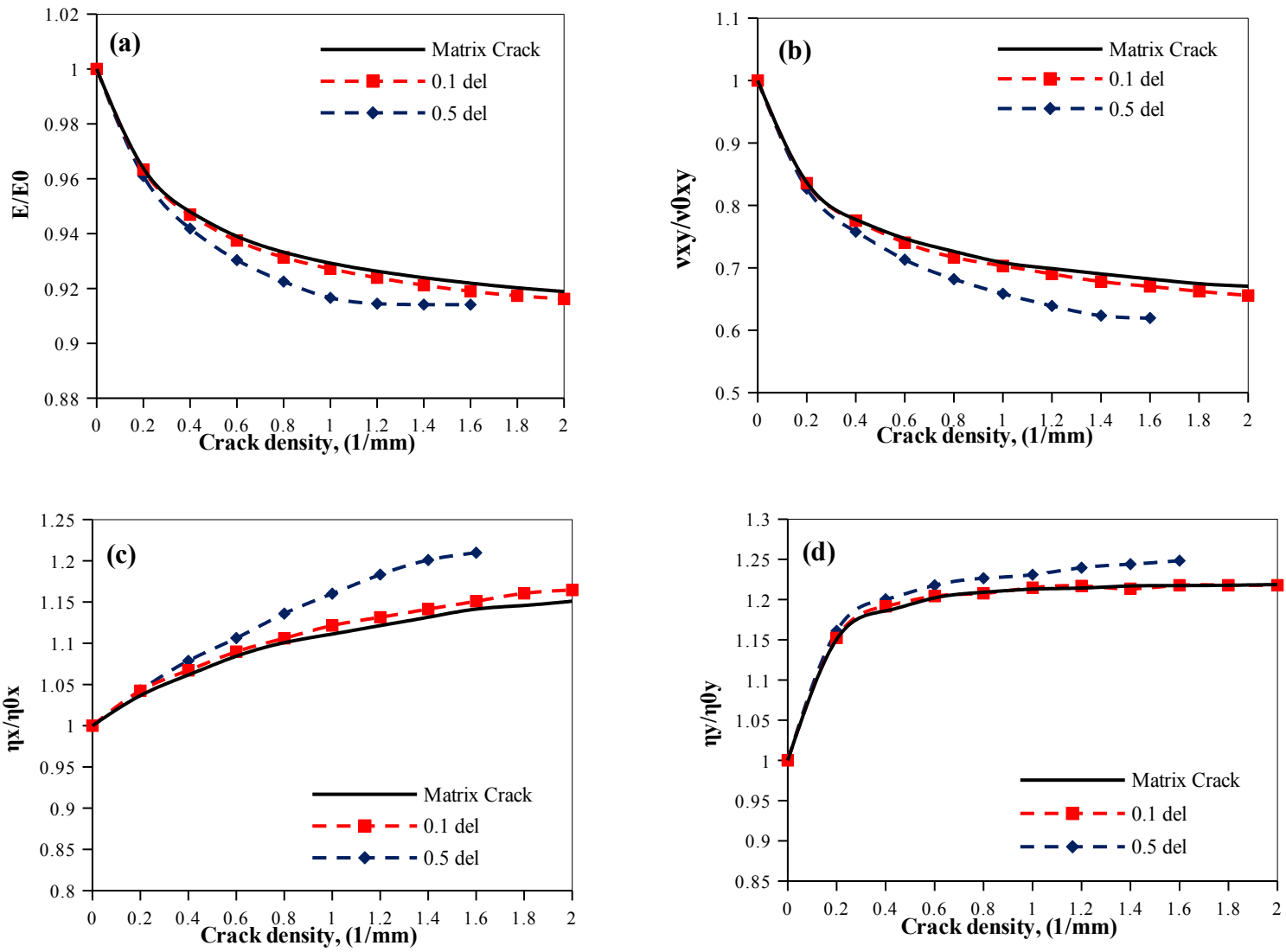

Fig. 8 Comparison of the variation of the properties due to matrix cracking and delamination with l_d= 0.1 and l_d=0.5 in the angle-ply laminate$[90/30_2]_s$ subjected to bending loading; a) Longitudinal flexural modulus, b) Poisson's ratio, c) longitudinal mutual coefficient, and d) transverse mutual coefficient

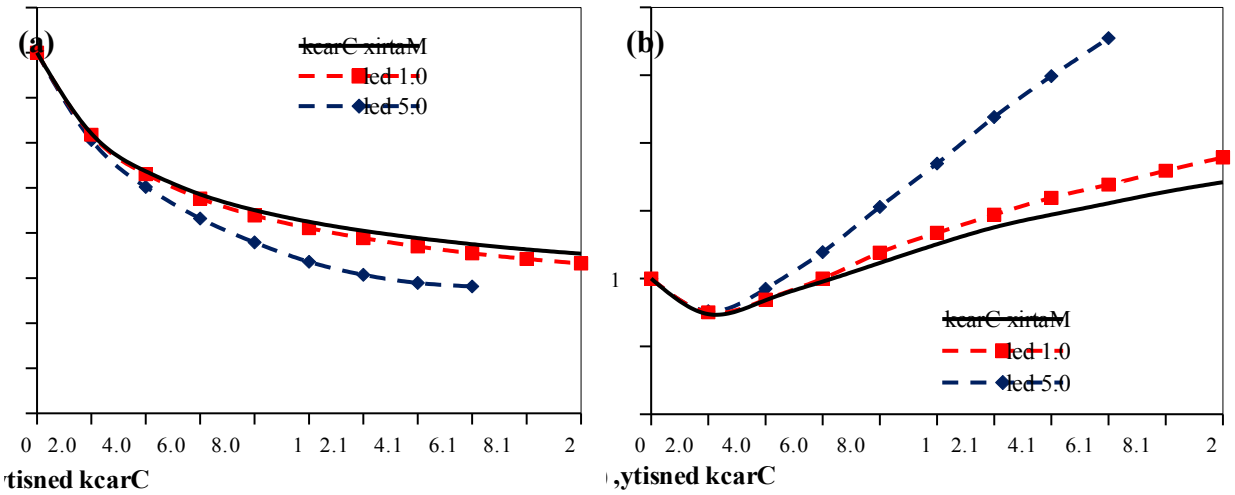

Fig. 9 Comparison of the variation of the properties due to matrix cracking and delamination l_d= 0.1 and l_d=0.5 in the angle-ply laminate $[60/-60]_s$subjected to bending loading a) Longitudinal flexural modulus, and b) Poisson's ratio

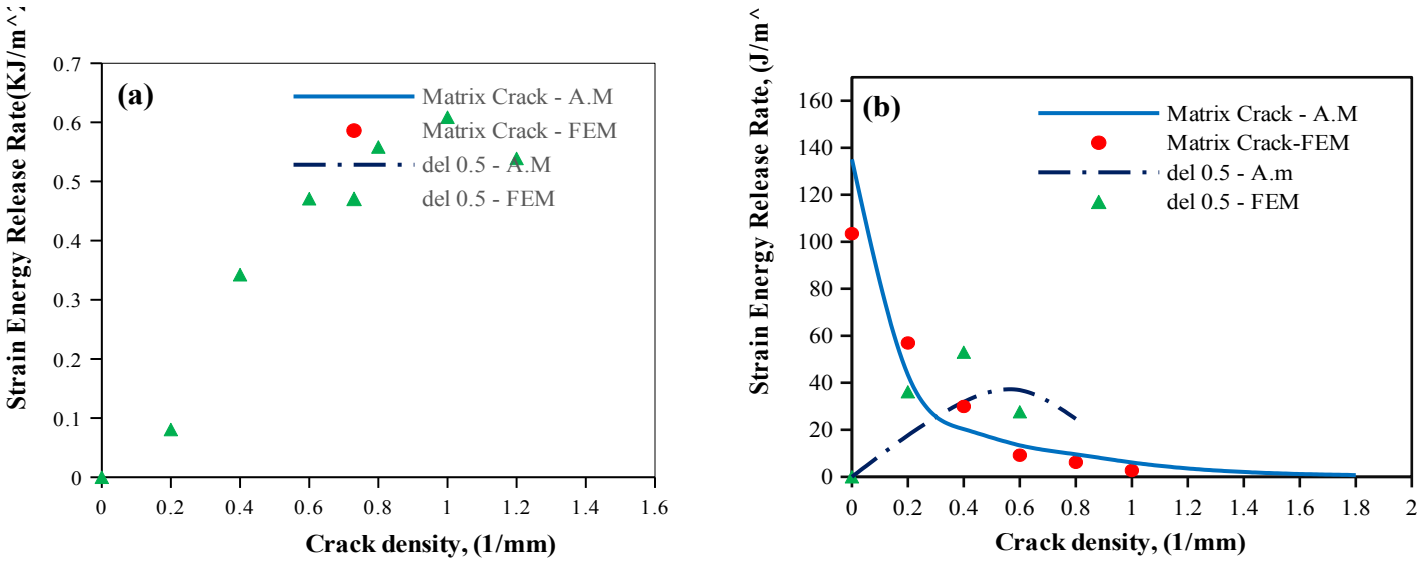

Fig. 10 A comparison of the variation of the SERR due to matrix cracking and induced delamination with l_d= 0.1 and l_d=0.5 between the numerical and analytical models a) $[90/0]_s$, and b) $[90_2/0_2]_s$

Table 1. Mechanical properties of the composite ply[12]

$E_1(GPa)$	$E_2(GPa)$	v_{12}	$G_{12}(GPa)$	v_{23}
104	6.14	0.4	0.5	0.45

Table 2. Comparison of the force required for the initiation delamination and matrix cracking in cross-ply laminates between the proposed model and the existing experimental results[25]

	Laminate					
	$[90_2/0_7/90_2]$		$[90_3/0_7/90_3]$		$[90_4/0_7/90_4]$	
	Load (N)		Load (N)		Load (N)	
Crack Number	Matrix Crack (EXP)	Delamination (P.S)	Matrix Crack (EXP)	Delamination (P.S)	Matrix Crack (EXP)	Delamination (P.S)
1	110	2224.43	101	1452.84	98	1254.49
2	115	1274.58	120	754.43	145	668.35
3	121	779.74	140	517.64	151	468.02
4	153	661.97	151	405.47	180	364.48
5	175	547.95	168	336.93	215	303.57
6	180	465.98	220	292.75	250	262.9
7	208	419.04	261	265.09	290.46	235.33
8	230	378.23	296.38	248.63		
9	240	346.98				
10	245	334.35				
11	280	318.36				
12	298	305.24				
13	315.7	284.85				